## Supporting Information

# Cavity Catalysis by Cooperative Vibrational Strong Coupling of Reactant and Solvent Molecules

*Jyoti Lather, Pooja Bhatt, Anoop Thomas, Thomas W. Ebbesen,\* and Jino George\**

anie_201905407_sm_miscellaneous_information.pdf

# Supporting Information

*para*-nitrophenyl acetate (PNPA) and tetrabutylammonium fluoride (TBAF) were purchased from Sigma-Aldrich. HPLC grade ethyl acetate ($^{12}$C=O), anisole and methanol (Merck Life Science) and ethyl acetate-1,2-$^{13}$C$_2$ (99 atom % $^{13}$C=O)(Sigma-Aldrich)were used as such for the experiments. Ester solvolysis of PNPA in mild basic condition of TBAF was carried out by mixing 0.1M PNPA (18mg PNPA in 1mL $^{12}$EtOAc) and 0.1M TBAF (31.5mg in 1mL methanol). Fresh solutions were used for each experiment. The reactant (0.1M PNPA) and the reagent (0.1M TBAF) are mixed in 9: 1 ratio, in a 4 mL glass vial and 300 μL of this reaction mixture was injected immediately into the FP cavity with a standard disposable syringe. Final concentrations of PNPA and TBAF are 0.1M and 0.01M respectively. The rate of the reaction is followed by observing the absorbance at 407 nm and kinetic data are plotted by observing the system up to 300 seconds.
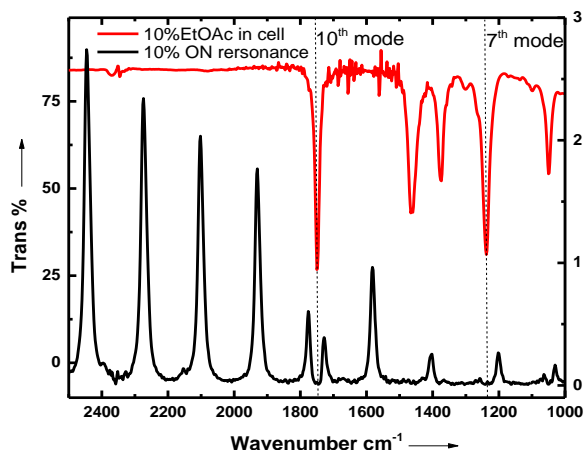


**Figure S1**: IR transmission spectra of PNPA in 10% $^{12}$EtOAc (red trace) and the corresponding P+ and P- formed by coupling to the 10$^{th}$ cavity mode (black trace).

Demountable flow cell with BaF$_2$ windows was purchased from Specac Ltd. UK and used for the studies. Mylar spacers with 18 μm thickness was used for the cell as well as the cavity experiments. 4 mm thick BaF$_2$ windows was coated with 10 nm Au film by thermal evaporation method and 100 nm of SiO$_2$ passivating layer is deposited by RF sputtering onto the Au film. IR spectra were recorded by Perkin-Elmer FT-IR spectrophotometer (*Spectrum 1*). Cavity modes are

tuned precisely by tightening or loosening the four precision screws on different corners of the flow cell. Free spectral range (FSR) is measured in every case by taking the average of 6 cavity modes of an empty cavity and by back calculation we assure ON resonance situation from the beginning of the injection of the reaction mixture (Figure S1; Table S1). Calculation of the FSR can be done by using the formula; $k(cm^{-1}) = \frac{10000}{2nL}$, where *n* is refractive index (RI) of medium and *L* is the length between the mirrors (μm). RI of the solution was estimated a priori for achieving ON resonance situation and the actual FSR is measured to cross-check after the completion of the reaction, assuming that the product formed will not change the RI of the medium during the course of the reaction, a reasonable assumption since the reactant concentration is 1, 000 times lower than the solvent medium. After setting the empty cavity FSR, system is kept at rest for 30 minutes. Both the reactant and the reagent are maintained at 30°C in a water bath for equilibration and the reaction mixture was injected into the cavity followed by observing the kinetic traces at 407 nm in a UV-Vis spectrophotometer (Carry 5000).
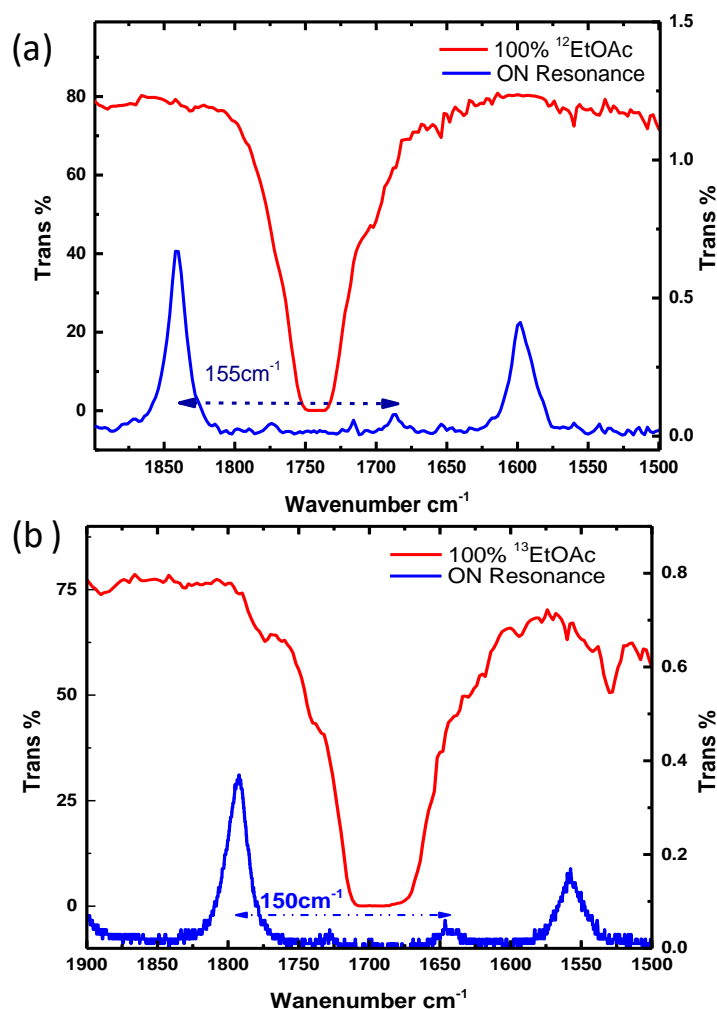
**Figure S2**: IR spectra ofcarbonyl band (red trace) and the corresponding P+ and P- formed(blue trace) by coupling to the 10th mode of cavity (a) $^{12}$EtOAc and (b) $^{13}$EtOAc.

IR spectra of EtOAc exhibit carbonyl $^{12}$C=O and $^{13}$C=O stretching mode at 1750 cm$^{-1}$ and 1706cm$^{-1}$, respectively. Coupling the 10th mode of the cavity to the carbonyl band of $^{12}$EtOAc resulted in a Rabi Splitting energy of 155 cm$^{-1}$ with P+ and P- at 1840 cm$^{-1}$ and 1685 cm$^{-1}$ respectively (Figure S2a).Similarly, $^{13}$EtOAc coupling of carbonyl band resulted in a Rabi Splitting energy of 150cm$^{-1}$with P+ and P- at 1792 cm$^{-1}$ and 1642 cm$^{-1}$(Figure S2b). The number of molecules calculated from the concentration and volume occupied (3μL) is roughly 10$^{15}$ for PNPA and 10$^{18}$ for ethyl acetate molecules.

Next, we compared the change in the solvent mixture with respect to the reaction rate. Here, the cell was maintained at the same pathlength and kinetics was measured by varying the

concentration of [12]EtOAc from 25% to 100% in a step of 25%. Anisole was taken as the mixing solvent due to similar polarity as that of [12]EtOAc. The reaction rate for varying concentration of [12]EtOAc is plotted in Figure S3. It should be noted that the rate increase is negligible compared to the VSC condition as mentioned in the Figure 4b.
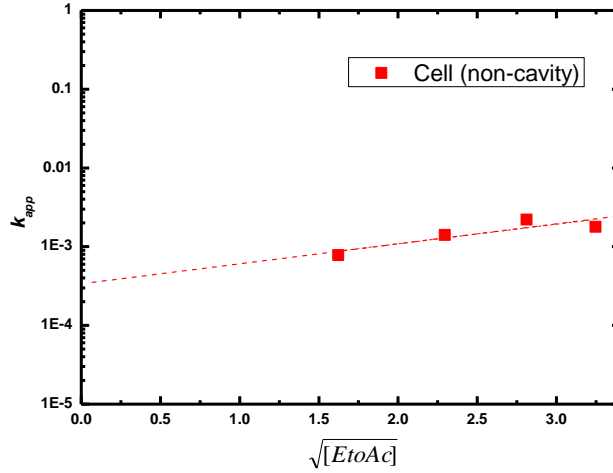


**Figure S3**: Semi-logarithmic plot of apparent rate verses square root of concentration of [12]EtOAc.

**Table S1**: FSR of the empty cavity and reacting medium inside the QED reactor and the corresponding rate as plotted in Figure 3d.

| s.no. | Empty cavity free spectral range | FSR after injecting reaction mixture | K(reaction rate)s$^{-1}$ |
|---|---|---|---|
| 1 | 240.46 | 174.9 | $2.54 \times 10^{-2}$ |
| 2 | 239.91 | 175.5 | $0.72 \times 10^{-2}$ |
| 3 | 240.29 | 175.3 | $1.61 \times 10^{-2}$ |
| 4 | 236.96 | 172.9 | $0.44 \times 10^{-2}$ |
| 5 | 233.9 | 171.3 | $0.40 \times 10^{-2}$ |
| 6 | 245.13 | 177.9 | $0.33 \times 10^{-2}$ |
| 7 | 230.5 | 168.2 | $0.33 \times 10^{-2}$ |
| 8 | 251.3 | 183.5 | $0.16 \times 10^{-2}$ |

**Transfer Matrix Method (TMM) simulation:**

Transfer Matrix Method (TMM) simulation predict approximately the cavity modes, by solving Maxwell equation for multiple layers having different refractive indices during the light propagation. Here, we constructed a multilayer index medium with pure Au mirrors (thickness; approx. 10 nm), dielectric $SiO_2$ (100 nm; refractive index data was taken from https://refractiveindex.info). The mirror spacing are tuned to achieve strong coupling condition with carbonyl stretching mode. 10th mode of the cavity is coupled to the C=O stretch and the bulk RI was taken approx. as 1.37.
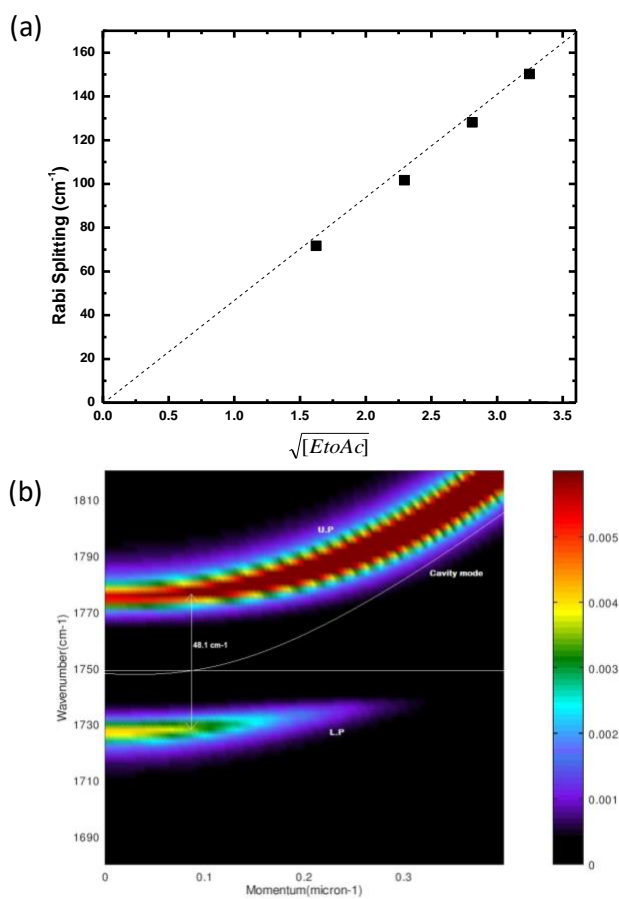


**Figure S4**: (a) Rabi splitting verses square root of concentration of [12]EtOAc; C=O stretching band is at $\omega_0$=1750 cm-1 and (b) the dispersion curve for carbonyl VSC for 10% [12]EtOAc.

**Transmission spectra of EtOAc in a single mirror (half-cavity) cell:**

Transmission spectra of pure EtOAc molecules in half-cavity (Figure S5; one of the BaF2 substrate coated with 20 nm Au film) shows the fundamental C=O stretching mode. This clearly indicate that a single mirror (half-cavity) structure cannot impart strong interaction in the system.
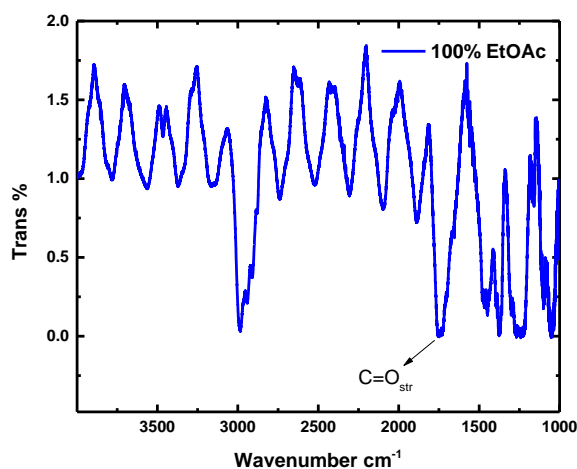


**Figure S5**: IR spectra of EtOAc with one BaF$_2$ substrate having 20 nm Au film with 18 μm spacer.

**Mechanism of ester hydrolysis:**

Base catalysed ester hydrolysis is predicted to follow a B$_{AC2}$ mechanism, implying that the nucleophile attack on the electron deficient carbonyl carbon atom and proceeds through a tetrahedral transition state as proposed in the Scheme S1. First, the nucleophile attack is the rate determining step and secondly, acyl bond breaking is considered to follow the TS, leading to the formation of the product. As predicted theoretically in a few cases, *para*-nitro phenoxide (PNP-) is a better leaving group that make the system to follow a concerted path. Here, PNPA hydrolysis is purely dependent on the stability of the TS that can be controlled by the surrounding solvent
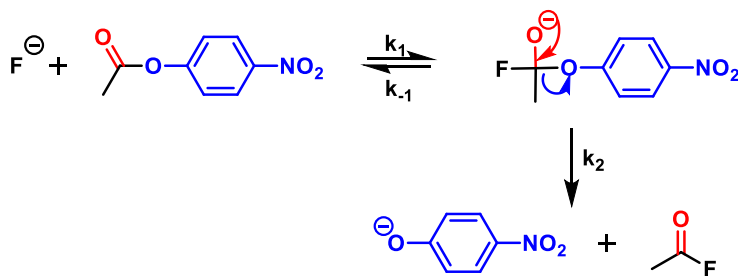


molecules.

**Scheme S1**: Mechanism of the hydrolysis of PNPA.

6

Formation of PNP- can be monitored using a UV-VIS spectrophotometer both in non-cavity as well as in cavity (Figure S6) gives a direct access to the relative concentration of the product formed during the course of the reaction.
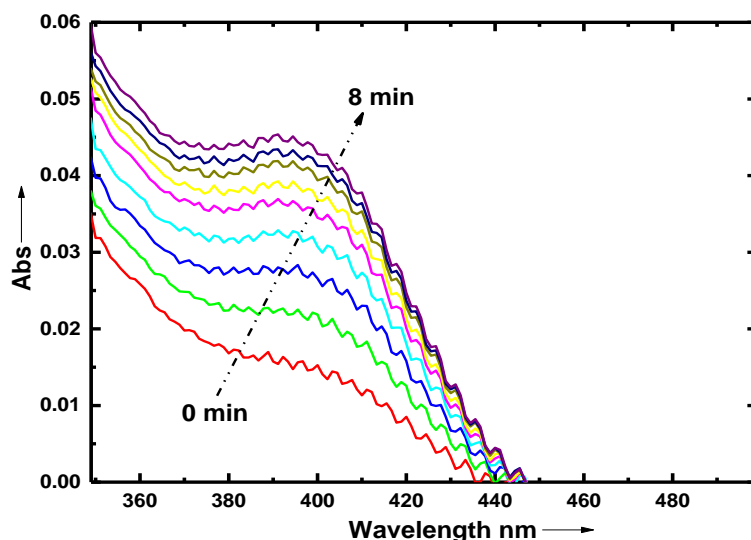


**Figure S6**: Temporal evolution of PNP- inside the cavity in the UV- Visible region.

**Thermodynamic parameters from Eyring equation:**

Reaction rate can be correlated with temperature to extract the thermodynamics parameters using Eyring equation.

$$k = \frac{k_B T}{h} exp\left(\frac{-\Delta H^{\neq}}{RT} + \frac{\Delta S^{\neq}}{R}\right)$$

Enthalpy $(\Delta H^{\neq})$ and entropy $(\Delta S^{\neq})$ of activation values can be calculated by plotting $\ln(k/T)$ vs. $(1/T)$. From fig 4a these values can be obtained in which slope $\frac{-\Delta H^{\neq}}{R}$ gives $(\Delta H^{\neq})$ and intercept $\ln\left(\frac{k_B}{h}\right) + \frac{\Delta S^{\neq}}{R}$ gives $(\Delta S^{\neq})$

<u>**From figure 4a:**</u>

<u>**Non-cavity:**</u>

$$\frac{-\Delta H^{\neq}}{R} = -6400.29 \text{ (slope)}$$

$$\Delta H^{\neq} = 53.2 \ kJmol^{-1}$$

$$\ln\left(\frac{k_B}{h}\right) + \frac{\Delta S^{\neq}}{R} = 15.23 \text{ (intercept)}$$

$$ln\left(\frac{k_B}{h}\right) = 23.76 \quad \text{(constant)}$$

$$\Delta S^{\neq} = -70.9 \, JK^{-1}mol^{-1}$$

**Cavity:**

$$\frac{-\Delta H^{\neq}}{R} = -943.77 \text{ (slope)}$$

$$\Delta H^{\neq} = 7.9 \, kJmol^{-1}$$

$$ln\left(\frac{k_B}{h}\right) + \frac{\Delta S^{\neq}}{R} = -1.04 \text{ (intercept)}$$

$$ln\left(\frac{k_B}{h}\right) = 23.76 \quad \text{(constant)}$$

$$\Delta S^{\neq} = -206.2 \, JK^{-1}mol^{-1}$$

$$\Delta\Delta H^{\neq} = \Delta H^{\neq} cavity - \Delta H^{\neq} cell = \mathbf{-45.3 \, kJmol^{-1}}$$

$$\Delta\Delta S^{\neq} = \Delta S^{\neq} cavity - \Delta S^{\neq} cell = \mathbf{-135.3 \, JK^{-1}mol^{-1}}$$

$$\Delta\Delta G^{\neq} = \Delta G^{\neq} cavity - \Delta G^{\neq} cell = \mathbf{-5.03 \, kJmol^{-1}} \text{ at 298 K.}$$